



HAL
open science

New insights into sorption and desorption of organic phosphorus on goethite, gibbsite, kaolinite and montmorillonite

Issifou Amadou, Michel-Pierre Faucon, David Houben

► **To cite this version:**

Issifou Amadou, Michel-Pierre Faucon, David Houben. New insights into sorption and desorption of organic phosphorus on goethite, gibbsite, kaolinite and montmorillonite. *Applied Geochemistry*, 2022, 143, pp.105378. 10.1016/j.apgeochem.2022.105378 . hal-03711164

HAL Id: hal-03711164

<https://hal.science/hal-03711164v1>

Submitted on 1 Jul 2022

HAL is a multi-disciplinary open access archive for the deposit and dissemination of scientific research documents, whether they are published or not. The documents may come from teaching and research institutions in France or abroad, or from public or private research centers.

L'archive ouverte pluridisciplinaire **HAL**, est destinée au dépôt et à la diffusion de documents scientifiques de niveau recherche, publiés ou non, émanant des établissements d'enseignement et de recherche français ou étrangers, des laboratoires publics ou privés.

1 **New insights into sorption and desorption of organic phosphorus on goethite,**
2 **gibbsite, kaolinite and montmorillonite**

3 Issifou Amadou^{a*}, Michel-Pierre Faucon^a and David Houben^a

4 ^a AGHYLE (SFR Condorcet FR CNRS 3417), UniLaSalle, 19 Rue Pierre Waguet, 60026 Beauvais,
5 France

6 *corresponding author: Issifou.Amadou@unilasalle.fr

7 **Highlights**

- 8 • Mineral properties and organic P (OP) characteristics affected OP (de)sorption
- 9 • Myo-inositol hexakisphosphate had higher adsorption than the other OP forms
- 10 • Organic P showed contrasted adsorption capacities relative to inorganic P forms (IP)
- 11 • Fe and Al oxides exhibited highest adsorption capacity compared to clay minerals
- 12 • Organic P was more desorbed from clays minerals than from Fe and Al oxides

13 **Abstract**

14 With the increasing use of organic resource for P fertilization, the adsorption and desorption dynamics
15 of various organic phosphorus (OP) forms remain an important gap of knowledge to bridge in order to
16 improve P availability. In this study, we examined the adsorption and desorption dynamics of various
17 OP (myo-inositol hexakisphosphate, myo-IHP; glycerophosphate, GLY; and glucose-6-phosphate,
18 G6P) compounds to and from several soil minerals including Fe and Al oxides (goethite and gibbsite,
19 respectively) and clays minerals (kaolinite and montmorillonite). Overall, myo-IHP was the most
20 adsorbed form followed by G6P and then GLY which reflected that OP adsorption increased according
21 to the number of phosphate groups and/or the size of the organic molecule. Fe and Al oxides showed
22 higher OP adsorption capacity than clays, as adsorption followed the trend kaolinite < montmorillonite
23 < goethite <<<< gibbsite.

24 Desorption experiments revealed that the adsorption was not fully reversible as only 30% could
25 easily desorbed. On Fe and Al oxides, G6P and GLY were more desorbed than myo-IHP while the
26 opposite trend was found on clay minerals. In addition, OP desorption from soil minerals followed the
27 trend gibbsite < goethite < kaolinite < < montmorillonite. The clay-OP complex released P rapidly but
28 over a short period of time, whereas the Fe- and Al-OP complex released P slowly but over a longer
29 period of time. The comparison between the P adsorption and desorption properties of montmorillonite
30 and other soil minerals are only valid for the K-saturated montmorillonite used here. The results could
31 be different if the montmorillonite were saturated with Al or Ca. By deciphering the interactions between
32 soil minerals and the predominant forms of OP in soils and organic fertilizers, our results provide new
33 insights for the sustainable management of P in agroecosystems.

34 **Keywords:** Adsorption; desorption; organic phosphorus; phosphorus availability; soil fertility

35 **1. Introduction**

36 Phosphorus (P) is one of the essential nutrients required for plant growth and an important driver of
37 agroecosystem productivity (Hu et al., 2020a; Ruttenberg and Sulak, 2011). Due to its low solubility
38 and high affinity for mineral surfaces (Roy et al., 2017; Tisdale and Nelson, 1966), P availability is
39 limited in agricultural soils and rarely sufficient for optimum growth and development of crops. On the
40 other hand, accumulation of P in the soil increases the risk of P leaching and runoff, consequently leading
41 to eutrophication of surface waters (Hansen et al., 2002). Therefore, with the increasing use of organic
42 resources as P fertilizers (Amadou et al., 2021), a sustainable and efficient use of organic P (OP)
43 fertilizers is of utmost importance to secure future crop production and reduce environmental
44 hazard (Faucon et al., 2015). However, most of the research investigating the fate of P applied to the soil
45 has focused on inorganic P (IP) so far, showing that most of it was adsorbed onto iron (Fe) and aluminum
46 (Al)-oxides and clays minerals (Celi et al., 2000, 1999) or precipitated with Ca (Houben et al., 2011;
47 Urrutia et al., 2013). In contrast, the fate of OP has been disregarded so far even though it is now clear
48 that these forms of P can be at least as available as IP (Amadou et al., 2021; Kahiluoto et al., 2015).

49 Organic P can be mineralized along with plant uptake and/or be protected by organic substances from
50 adsorption, even in the long term (Huang and Zhang, 2012). However, the adsorption mechanisms of
51 OP and the factors that affect sorbing processes remain poorly understood (Yan et al., 2014) and there
52 is still a lack of knowledge about their contribution to plant nutrition (Faucon et al., 2015).

53 Organic P in soil-plant-system comes from both soil and organic waste sources (e.g. manure,
54 compost, sludge, biochar, ...) (Fuentes et al., 2006). The major OP compounds from soil and organic
55 wastes include myo-IHP (Turner et al., 2002; Vincent et al., 2013), GLY (Doolette et al., 2011; Newman
56 and Tate, 1980) and G6P (Deiss et al., 2018; Giles et al., 2011). Each form differs from the others by its
57 P content, P bond type and molecular size. They may constitute large fractions of the total P in soils
58 (Monbet et al., 2009), especially in organic waste-amended soils (Khare et al., 2004). It has been shown
59 that adsorption of OP compounds increases with the number of P groups. Therefore, with six phosphate
60 groups, myo-IHP has a high charge density and would undergo a strong interaction with the soil
61 (Anderson and Arlidge, 1962; Celi et al., 1999). This higher accumulation of myo-IHP through
62 adsorption limits P acquisition by plants from this source. The size and molecular structure of OP forms
63 generally affect their adsorption capacity. The G6P adsorption density and rate is higher than myo-IHP
64 and adenosine triphosphate (ATP) as a result of its lower molar mass (Giaveno et al., 2008). However,
65 Goebel et al., (2017) reported that G6P is potentially more available than myo-IHP and ATP.

66 After adsorption, the ability of soil minerals to release P in soil solution determines P availability
67 for plants but also loss of P in both surface runoff and subsurface flow (Sharpley et al., 2001). Several
68 authors have suggested that P from mineral-P complexes is not available to plants because of their very
69 limited desorption (Barrow, 1986; Bollyn et al., 2017; Guzman et al., 1994; Lagos et al., 2016). For
70 instance, Bollyn et al., (2017) showed that after several cycles of desorption, less than 5% P desorbed
71 from myo-IHP-goethite complexes. Similar results by Lagos et al., (2016) showed limited desorption of
72 myo-IHP (<3% P) from gibbsite. On the other hand, there is also experimental evidence that P can
73 desorb significantly from minerals to be available to plants and runoff (Andrino et al., 2019; Parfitt,
74 1979). However, in all of these studies cited above, the form of P used was exclusively IP with very
75 limited consideration for important OP pools such as IHP, GLY or G6P. Furthermore, the soil minerals
76 used were in most cases Fe oxides (namely goethite) while Al oxides and clay minerals were much less

77 investigated. To our knowledge, no study has evaluated and compared P desorption from the main OP
78 compounds (IHP, GLY, and G6P) that were adsorbed onto the main soil minerals (Fe and Al oxides,
79 and clay minerals). There is a need to bridge this gap of knowledge to identify the properties that govern
80 OP adsorption and desorption processes and gaining insight into the behavior of OP compounds at the
81 surface of soil minerals.

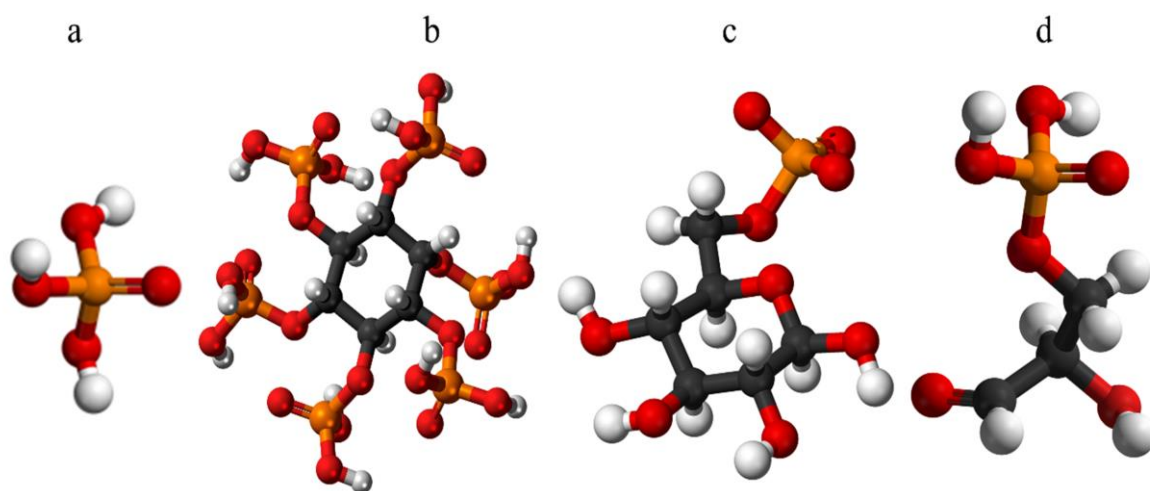
82 In sum, extensive research has evaluated the adsorption of different individual sources of
83 organic and inorganic P to soils or to individual soil minerals. However, no study has evaluated and
84 compared P desorption from the main OP compounds that were adsorbed onto the main soil minerals.
85 The aim of our study was to elucidate the dynamics of adsorption and desorption of several forms of OP
86 on several representative soil minerals. More specifically, we aimed at determining the drivers of
87 adsorption and desorption of OP on soil minerals. For this purpose, we studied the adsorption of three
88 OP compounds, myo-inositol hexakisphosphate (myo-IHP), glycerophosphate (GLY) and glucose-6-
89 phosphate (G6P) and one inorganic compound (KH_2PO_4 , IP) on Fe and Al oxides (goethite and gibbsite,
90 respectively) and on clay minerals (kaolinite and montmorillonite). Organic P sources were chosen
91 based on their predominance in both soils and organic inputs and their contrasted chemical properties.
92 We assume that the selected Fe, Al oxides and clay minerals, abundant in the soils, will present different
93 capacities of adsorption and desorption due to their chemical properties.

94 **2. Materials and methods**

95 2.1. Organic P forms and individual soil minerals

96 Three organic P (OP) compounds, myo-IHP, GLY, G6P and one IP (KH_2PO_4) (Fig.1) were selected
97 based on their predominance in organic wastes and soils and their contrasted properties (type of P bonds,
98 different molecular sizes). The individual soil minerals were selected to be representative of the
99 predominant soil minerals involved in P adsorption in soils. Four individual soil minerals were used.
100 Goethite [$\text{FeO}(\text{OH})$] and gibbsite [$\text{Al}(\text{OH})_3$] were chosen as representative of Fe and Al oxides;
101 kaolinite and montmorillonite were selected as clay minerals, particularly 1:1 phyllosilicate and 2:1
102 phyllosilicate respectively. The minerals used have different specific surface areas (SSA) and points of

103 zero charge (PZC). The SSA of the minerals used are as follows: goethite ($46 \text{ m}^2 \text{ g}^{-1}$), gibbsite ($120\text{-}364$
104 $\text{m}^2 \text{ g}^{-1}$), kaolinite ($19 \text{ m}^2 \text{ g}^{-1}$) and K-montmorillonite ($83 \text{ m}^2 \text{ g}^{-1}$) and their PZCs were: goethite (7.04),
105 gibbsite (9.3), kaolinite (4.5) and montmorillonite (2.5), as previously reported by other authors (He et
106 al., 1994; He and Zhu, 1997; Ruttenberg and Sulak, 2011; Shang et al., 1990; Yan et al., 2014). All
107 minerals were obtained from Sigma-Aldrich Chemie S.a.r.l. and VWR (France) for experimentation (see
108 supplementary data references in supplementary data (Table S1) for mineral references)



109
110 Fig.1. Chemical structure of potassium dihydrogen phosphate, IP (a), myo-inositol hexakisphosphate,
111 IHP (b), β -D-Glucopyranose-6-phosphate, G6P (c) and Glycerol phosphate, GLY(d).

112 2.2. Adsorption Experiments

113 Triplicate batch experiments were conducted to understand the interactions between OP forms and soils
114 minerals at different P concentrations. We used standard P adsorption procedure proposed by Nair et
115 al., (1984). Prior to adsorption, 80mg of each soil mineral were weighed and transferred to 50 mL
116 polypropylene centrifuge tubes. Then, 20 ml of 0.1 M KCl were added and the tubes were shaken for 24
117 hours at 25°C to sufficiently hydrate the adsorption sites on the minerals. The pH was maintained at 5.5
118 ± 0.05 by adding 0.1 M HCl or NaOH solution. Six P concentrations (0, 4, 8, 16, 40, 75 and 100 mg L^{-1})
119 were used for each P forms. Phosphorus stock solutions of each OP were prepared under the same
120 conditions of 0.1 M KCl at pH 5.5. KCl was used as electrolyte to mimic the environmental condition

121 and adjust ionic strength of the solution. To start the adsorption, 20 ml of solution containing each
122 concentration of P were pipetted into tubes containing the soil particles. The control experiment was the
123 same but without P. The final volume was 40 mL and the concentration of particles in this final volume
124 was 2 g L⁻¹. In each tube, some drops of hexanol were added to suppress microbial activities. The final
125 samples were shaken on a mechanical shaker for 24 hours at 25°C and then centrifuged (3000 g for 15
126 minutes). After centrifugation, samples were immediately filtered through a 0.22-µm membrane syringe
127 filter. The filtrates were stored in a cold room until the P content was analyzed. Inorganic P was
128 determined colorometrically (Ohno and Zibilske, 1991). Organic P compound samples was hydrolyzed
129 to IP form before colorimetric determination by using the persulfate oxidation method (Peters and Van
130 Slyke, 1932). The quantity of P adsorbed was calculated as the difference between the initial amount of
131 P added and the remaining P amount in solution at the end of the adsorption experiment. Adsorption
132 maxima, capacity and other adsorption parameters were determined by fitting data to the non-linear
133 form of the Langmuir (1) and Freundlich (2) isothermal model (Crini et al., 2007; Langmuir, 1918):

$$134 \quad Q_{\text{ads}} = Q_m K_L [C_e / (1 + K_L C_e)] \quad (1);$$

135 where C_e is the concentration of P in the equilibrium solution (mg L⁻¹), Q_{ads} is the total amount of P
136 adsorbed, K_L is the affinity constant or binding energy (L mg⁻¹), and Q_m is the P adsorption maxima
137 (µg g⁻¹). The ability of soil minerals to resist a change in solution P concentration was measured as the
138 maximum adsorption buffer capacity: $MBC = K_L \times (Q_m)$; where K_L and Q_m are the binding-energy
139 related constant and maximum adsorption, respectively, in the Langmuir equation.

$$140 \quad Q_{\text{ads}} = K_F C_e^{1/n_F} \quad (2);$$

141 where Q_{ads} (µg g⁻¹) is the total amount of P adsorbed, C_e is the adsorbate equilibrium concentration in
142 solution, K_F (µmol L⁻¹) is adsorption capacity, and n_F (mmol L⁻¹) is Freundlich exponent.

143 2.3. Desorption kinetics experiments

144 Prior to desorption, the four soil minerals were loaded with the three OP compounds or IP. Solutions
145 containing 1 g P L⁻¹ in 0.1 M KCl at pH 5.5 were prepared using the different P compounds. Goethite,
146 gibbsite, kaolinite and montmorillonite was weighed in portions of 100 g into 1L bottles containing.

147 Then, 200 ml of 0.1 M KCl were added and the bottles were shaken for 24 hours at 25°C to sufficiently
148 hydrate the adsorption sites on the minerals. The pH was maintained at 5.5 ± 0.05 by adding 0.1 M HCl
149 or NaOH solution. To start the complex formations, each of the 1L bottles containing the soil minerals
150 was filled with 800 ml of P solutions. This was done in order to obtain all the mineral-P complexes, for
151 example for goethite we will have: goethite-IP, goethite-IHP, goethite-G6P and goethite-GLY and
152 similarly for the other minerals. In each 1L bottles containing both the soil minerals and P compounds,
153 some drops of hexanol were added to suppress microbial activities. The final samples containing in the
154 bottles were shaken on a mechanical shaker for 24 hours at 25°C and then centrifuged (3000 g for 15
155 minutes). The 1L bottles were distributed into several small 250-mL bottles, centrifuged, and the
156 supernatants were collected. Centrifugation was repeated until the maximum volume of supernatants
157 was removed. The produced P-loaded minerals was agitated in deionized water and frozen at -20°C. The
158 amounts of adsorbed P were determined using the same procedure as described in Section 2.2. The
159 amounts of adsorbed P ($\mu\text{gP g}^{-1}$) were similar to the Q_m values (Table 1) of the adsorption data
160 (Section 2.2) that were predicted by the Langmuir model.

161 Desorption kinetics experiments were initiated by adding 40 ml of 0.1 M KCl adjusted to pH
162 5.5 to 0.5g of the different minerals-P complex. Samples were shaken on a mechanical shaker at 25°C
163 at regular intervals (24h, 48h, 72h, 96h). After the first cycle (24h), the entire suspension was removed
164 and immediately filtered through a 0.22- μm membrane filter. A fresh 40 ml solution of 0.1 M KCl was
165 added to start the second cycle (48h). The same process was applied for the remaining cycles. The P
166 concentration in the supernatant was determined as described above. Desorption maxima and rate were
167 determined by fitting data to the non-linear form of the Elovich kinetic model (Bulut et al., 2008) (3):

$$168 \quad Q = A + B * \text{Ln}t \quad (3);$$

169 where q is the amount of P desorbed at time t , and A and B are the constants with $A = \frac{1}{\beta}$ and $B =$
170 $\frac{1}{\beta} \text{Ln} \alpha \beta$ (α and β are the constants in the original formula of Elovich equation). The A value (mgP kg^{-1})
171 in the Elovich equation is the amount of P desorbed in the first day of desorption ($q = A + B * \text{Ln} t$, $A = q$
172 when $t = 1$) and that B (mgP day^{-1}) is positively related with the P desorption rate as demonstrated in

173 the studies of (He and al. 1994). A and B values have been used to compare P release rate in different
174 soils (He and Zhu, 1997). The maximum desorption amount (D_m) was calculated as total amount P
175 desorbed.

176 2.4. Statistical analysis

177 All the Langmuir, Freundlich and Elovich model's parameters were evaluated by non-linear regression
178 method using function *nls* from *Package 'nlstools'* in R software. Nonlinear parameter estimates can be
179 obtained using different methods (Archontoulis and Miguez, 2015; Bates and Watts, 1988); the most
180 common is ordinary least squares, which minimizes the sum of squared error between observations and
181 predictions (Brown, 2001). The determination coefficient (R^2) for each parameter was used to measure
182 the goodness-of-fit. Apart from R^2 , standard errors (S.E.) were also used to determine the best-fitting
183 isotherm to the experimental data. The conceptual framework was performed using *correlate* and
184 *network plot* function in the latest development version of the *corr package* (Ahmed et al., 2021). This
185 generates a network graph of a correlation data frame in which variables that are more highly correlated
186 appear closer together and are connected by stronger paths. The proximity of points is determined using
187 multidimensional clustering.

188 3. Results

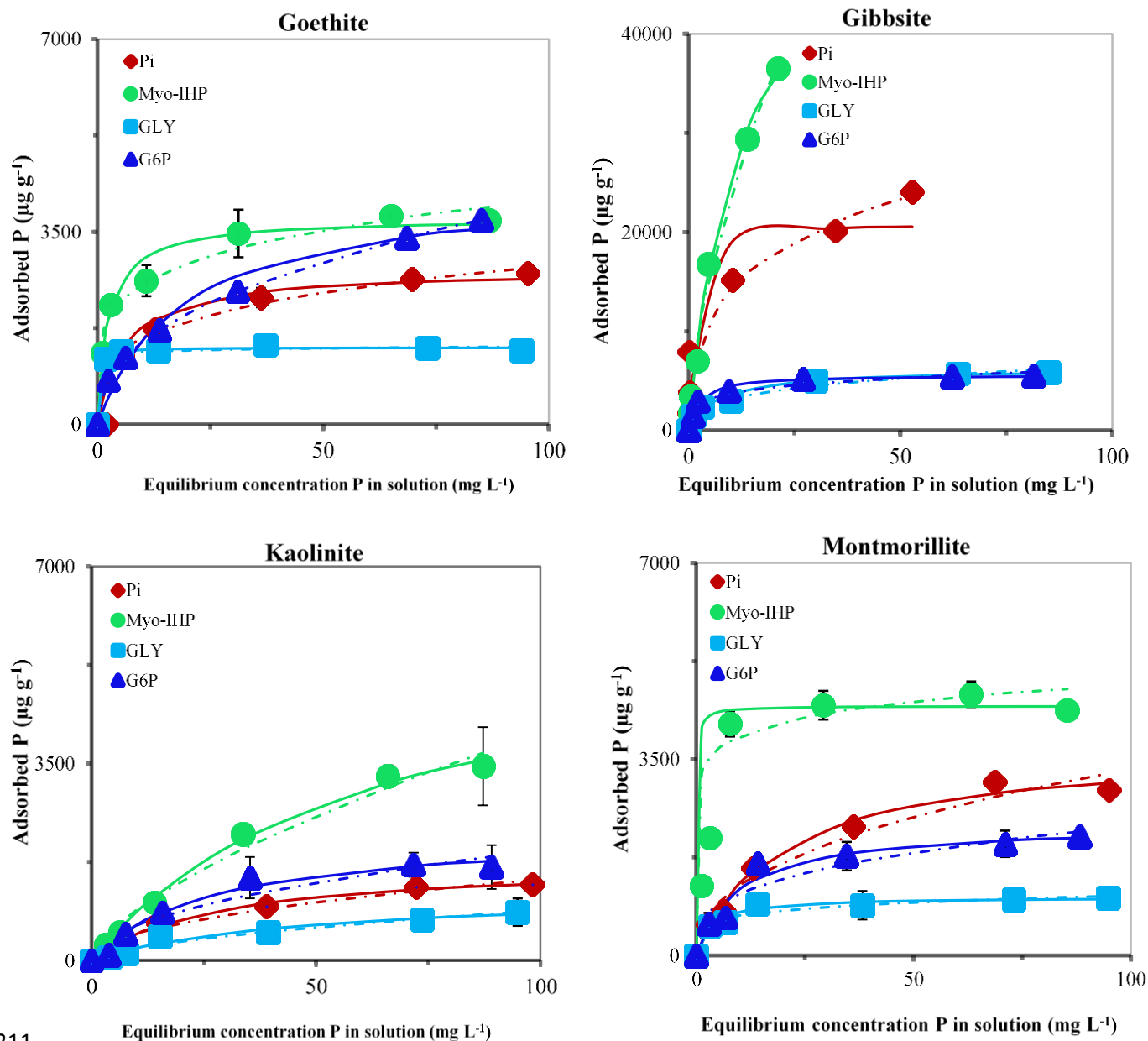
189 3.1. Dynamics of Organic Phosphorus Adsorption

190 3.1.1. Effect of OP forms on adsorption dynamics

191 Organic P adsorption differed for each specific OP compounds (Table 1). The strongest differences in
192 OP adsorbed among the different isotherms occurred with the greatest initial OP concentrations (Fig.
193 2). In addition, the magnitude of OP adsorption increased rapidly when the initial OP concentration was
194 low ($< 25 \text{ mg L}^{-1}$), but became relatively slow with increasing concentration (up to 40 mg L^{-1}). Each OP
195 compound had different adsorption characteristics onto the various soil minerals. The Q_m , i.e. maximum
196 OP adsorption capacity from the Langmuir equation (Table 1) ranged from $1045 \mu\text{g g}^{-1}$ to $56697 \mu\text{g g}^{-1}$,

197 indicating marked variations in the amount of OP adsorbed. Among the OP compounds, myo-IHP was
198 the most adsorbed form (3742-56697 $\mu\text{g g}^{-1}$) followed by G6P and then GLY (1045-6237 $\mu\text{g g}^{-1}$) (Fig.
199 2 and Table 1). The adsorption maxima of OP increased with increasing molar mass in this order: GLY
200 (172 g mol^{-1}) < G6P (260 g mol^{-1}) < myo-IHP (660 g mol^{-1}), which showed that the size of the molecule
201 would have favored the adsorption of OP compounds.

202 Compared to IP, a contrasted adsorption behavior of OP compounds was observed. The
203 adsorption dynamics followed the trend myo-IHP > IP > G6P > GLY, showing that myo-IHP was more
204 adsorbed than IP, which in turn was more adsorbed than the G6P and GLY forms (Fig. 2 and Table 1).
205 The K_L value, i.e. the binding energy between OP and minerals surfaces were highly variable. With the
206 exception of montmorillonite, GLY or G6P showed higher or equal binding strength compared myo-
207 IHP (Table 1). Our results showed that the adsorption dynamics of OP was strongly controlled by their
208 biogeochemical properties in the soil. The myo-IHP, GLY and G6P form showed a different adsorption
209 process from each other as well as from the IP form. In general, myo-IHP was found to be the most
210 adsorbed P form and GLY the least adsorbed form.



211

212

213 Fig. 2. Adsorption isotherms of OP forms by different soil minerals in 0.1 M KCl at pH 5.5: Symbols
 214 are data points, solid lines are Langmuir isotherms, and dashed lines are Freundlich isotherms. Gibbsite
 215 was different from other minerals because of the large difference in the maximum adsorption amount.
 216 Values of adsorbed quantities (Q_{ads}) and error bars (Se) are also provided as supplementary data (Table
 217 S2).

218 Table 1. Isotherm parameters of the Langmuir and Freundlich models for P adsorption.

Soil components	P Forms	Langmuir equation				Freundlich equation		
		Q _m (μg g ⁻¹)	K _L (L mg ⁻¹)	R ²	MBC (L Kg ⁻¹)	K _F	n	R ²
Goethite	IP	2810	0.16	0.97	450	848	3.77	0.99
	myo-IHP	3742	0.4	0.97	1497	1584	4.88	0.98
	GLY	1398	3.31	0.99	4626	1228	9.7	0.99
	G6P	4337	0.05	0.98	217	561	2.35	0.99
Gibbsite	IP	20949	0.99	0.91	20740	7158	3.31	0.96
	myo-IHP	56698	0.08	0.99	4536	5703	1.62	0.99
	GLY	6237	0.14	0.97	873	1584	3.26	0.98
	G6P	5588	0.4	0.98	2235	2254	4.58	0.96
Kaolinite	IP	1736	0.04	0.99	69	157	2.08	0.98
	myo-IHP	6082	0.02	0.99	122	197	1.53	0.98
	GLY	1222	0.02	0.96	24	57	1.68	0.96
	G6P	2295	0.04	0.98	92	198	2.01	0.92
Montmorillonite	IP	3709	0.05	0.99	185	465	2.34	0.97
	myo-IHP	4857	0.32	0.97	1554	1966	4.82	0.87
	GLY	1045	0.28	0.98	293	477	5.71	0.96
	G6P	2338	0.1	0.96	234	521	3.1	0.92

Q_m: maximum adsorption capacity, K_L: binding-energy related constant, R²: model fitting degree, MBC: maximum buffer capacity (ability of soil minerals to resist a change in solution P concentration).

219

220

221 3.1.2. Adsorption dynamics as affected by soil minerals

222 Isotherms of OP adsorption for the four tested minerals demonstrated that OP adsorption patterns of the

223 Fe and Al oxides (goethite and gibbsite, respectively) were very similar but quite different from that of

224 clays minerals (montmorillonite and kaolinite) (Fig. 1). Fe and Al oxides rapidly adsorbed OP and their

225 adsorption maximum was reached at a lower initial concentration than for clays. All tested minerals

226 fitted the Langmuir and Freundlich equation (Table 1). Adsorption capacity (K_F) of OP by soil minerals

227 followed the trend kaolinite < montmorillonite < goethite << Gibbsite (Table 1), showing a marked

228 variability between the adsorption capacities of the tested soil minerals. The Fe and especially Al oxides

229 exhibited the highest maximum adsorption capacity for all OP forms. The specific surface area (SSA)
230 of soil minerals may differently affect their ability to sorb OP compounds. Our result showed that the
231 larger the SSA of soil minerals, the greater their ability to sorb IP forms. However, this was not
232 consistent for the OP compounds. For instance, kaolinite showed greater myo-IHP adsorption than
233 goethite and montmorillonite despite its smaller specific surface area.

234 The K_L value, i.e. the binding-energy-related constant obtained from the Langmuir equation
235 varied in the following order clays \ll Fe and Al oxides (Table 1). The highest binding energy for
236 adsorbed OP was observed with goethite and the lowest with kaolinite. In addition, the maximum
237 buffering capacity of adsorption (MBC) of the Fe and Al oxides was much larger than for the clay
238 mineral (Table 1). Compared to IP, goethite and montmorillonite are more strongly bonded to OP;
239 however, the opposite was found on gibbsite and kaolinite, which bond IP more strongly than OP.
240 Therefore, despite the highest OP adsorption capacity of gibbsite, its interaction with OP would be less
241 strong than with IP. The results for the adsorption capacity and binding energy of montmorillonite are
242 only valid for the K-saturated montmorillonite used in this study. Al or Ca saturated montmorillonite
243 would result in different adsorption mechanisms. Fig. 6 illustrates a conceptual framework showing the
244 relationship between soil mineral properties (PZC, SSA) and Langmuir model adsorption parameters
245 (K_L and Q_m). A positive relationship was found between the ability of soil minerals to adsorb and
246 strongly bind OP and the chemical and physical properties of the soil minerals (PZC, SSA).

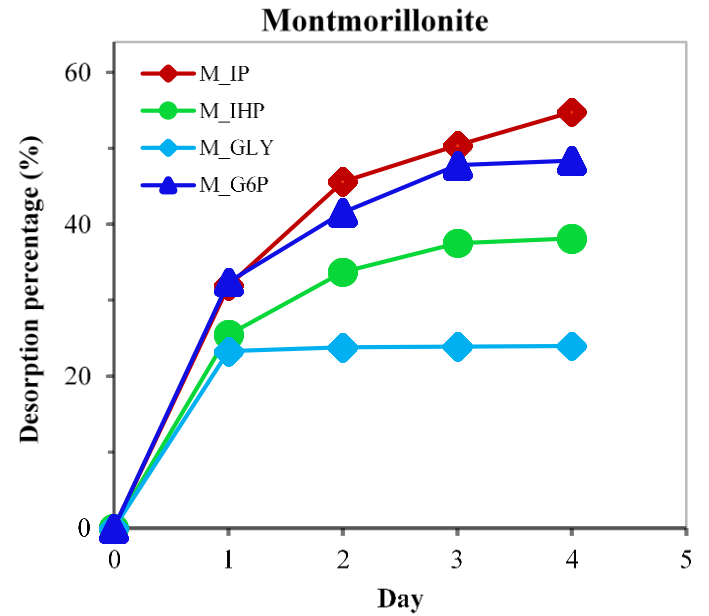
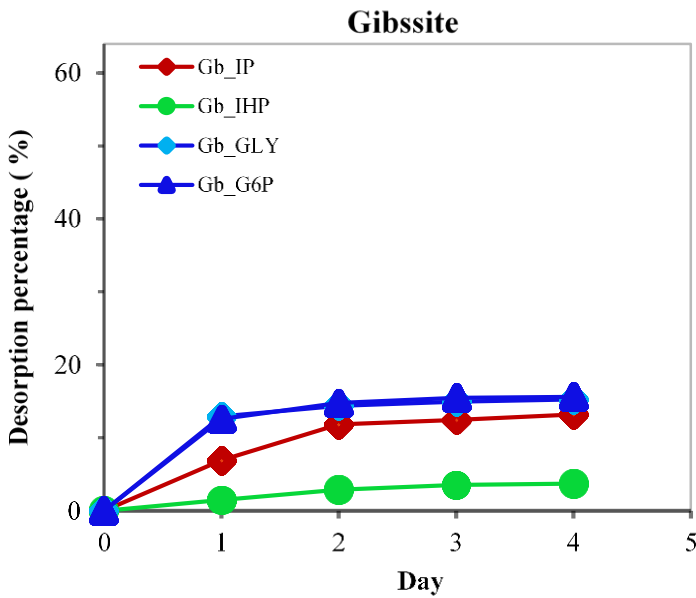
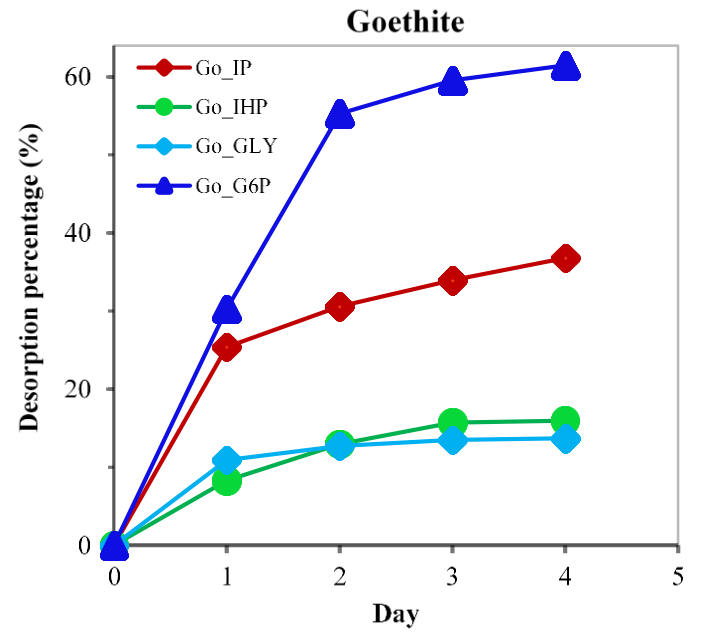
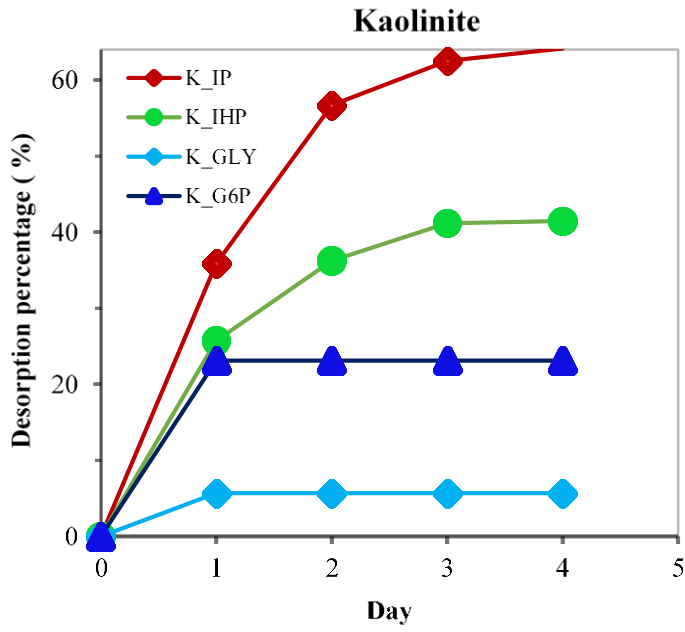
247 3.2. Dynamics of Organic Phosphorus Desorption

248 3.2.1. Role of OP compounds in desorption dynamics.

249 In general, OP desorption by KCl was well fitted with Elovich equation, with determination coefficient
250 from 0.91 to 0.99 (Table 2). In this study, KCl was found to desorb a variable portion of adsorbed OP
251 from the tested OP-mineral complexes. The portion of OP desorbed from all soil minerals was lower
252 than the initially adsorbed OP (Fig. 3 and Table 2) which indicates that the adsorption was not fully
253 reversible, as a large amount remained adsorbed. Overall, P desorption was high on the first day (up to
254 30%) and then slowed down from the second to the fourth day (Fig. 3 and Table 2).

255 The D_m values refer to the predicted maximum desorption capacity of OP obtained from the
256 Elovich model (Table 2). Organic P compounds showed different D_m trends by mineral type. Both G6P
257 and GLY showed higher D_m values (13%-56%) than myo-IHP (3%-14.44%) on Fe and Al oxides. On
258 clay minerals, the pattern was rather opposite, with myo-IHP desorption being higher than other OP
259 forms (Table 2). The desorption maxima of all of the OP compounds were 4% -56%, lower than those
260 of IP which were between 13 % to 70% (Table 2 and Fig. 3), showing a general lower desorption of OP
261 relative to IP. However, there were some exceptions with G6P and/or GLY which showed higher
262 desorption than IP on Fe and Al oxides. The amount of OP desorbed could be related to the strength
263 with which it was bound to soil minerals (adsorption parameter K_L). The Fig. 6 showed negative
264 correlations between D_m and K_L , indicating that the amount of OP desorbed tends to decrease with
265 increasing OP binding energy to the soil minerals.

266 The rate of OP desorbed per day (A) predicted by the Elovich model varied widely for each OP-
267 mineral complex (Table 2). Most of OP-minerals complexes showed lower desorption rates per day than
268 IP-minerals. In addition, the different OP-mineral complexes can be classified according to desorption
269 rates into three categories (Fig. 4): low desorption rate complexes (<5% per day) which include all the
270 OP desorbed from gibbsite and kaolinite; medium desorption rate complexes (10-20% per day)
271 including myo-IHP and G6P from montmorillonite and high desorption rate complexes (20% > per day)
272 which include only G6P from goethite (Fig. 3).



273

274

275 Fig. 3. Desorption kinetics of myo-IHP, GLY and G6P by 0.1 M KCl at pH 5.5 and at 25°C.

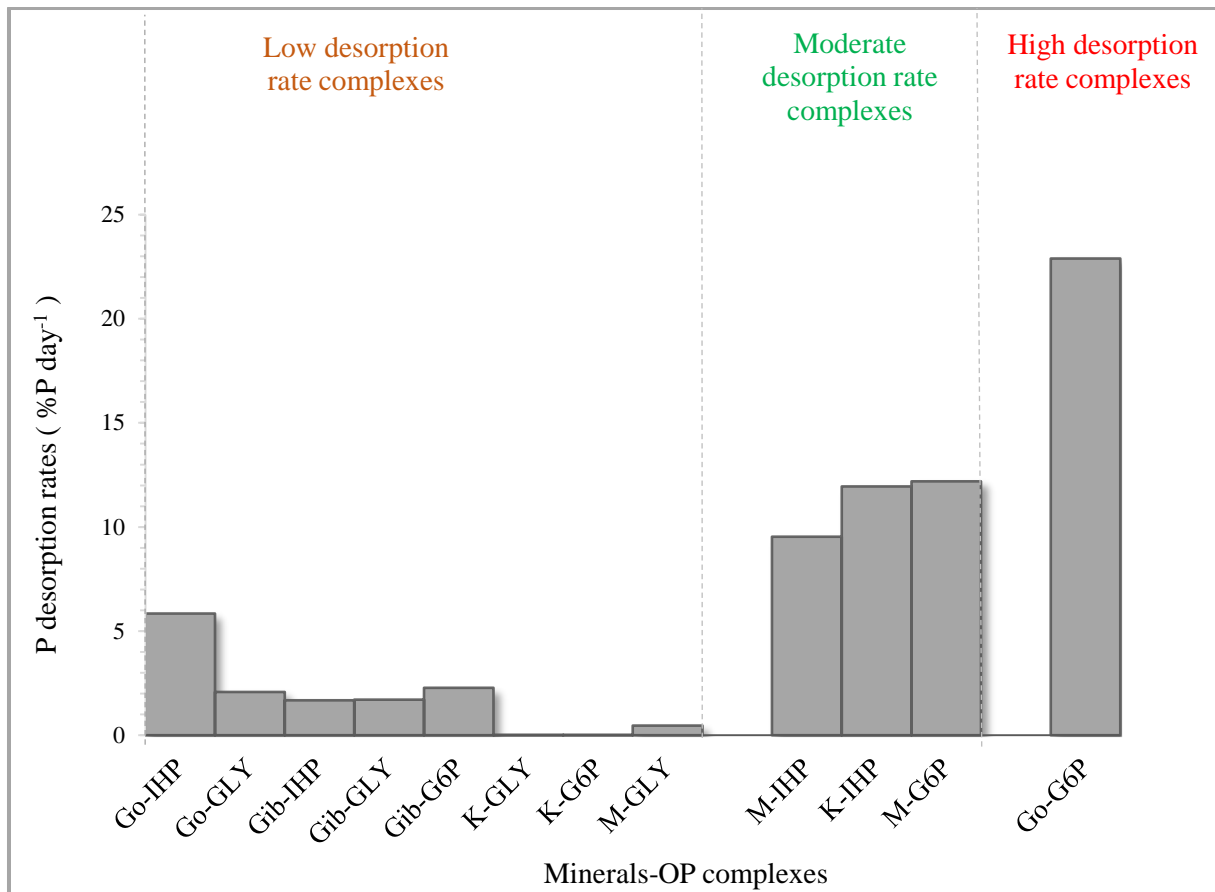
276 Table 2. Organic P desorption isotherm parameters of the Elovich model.

Soil components	P Forms	Elovich equation			
		Dm (%P g ⁻¹)	A (%P day ⁻¹)	B (%P g ⁻¹)	R ²
Goethite	IP	33	8	25	0.99
	myo-IHP	14	6	9	0.97
	GLY	13	2	11	0.97
	G6P	56	23	33	0.90
Gibbsite	IP	12	5	7	0.91
	myo-IHP	3	2	2	0.97
	GLY	15	2	13	0.98
	G6P	15	2	13	0.94
Kaolinite	IP	59	21	38	0.94
	myo-IHP	39	12	27	0.95
	GLY	6	0.01	6	0.98
	G6P	23	0.01	23	0.98
Montmorillonite	IP	49	16	33	0.99
	myo-IHP	36	10	26	0.96
	GLY	24	0	23	0.92
	G6P	45	12	33	0.97

Dm: maximum P desorption capacity, A: P desorption rate, B: amount of P desorbed in the first day of desorption in this study ($q = A + B * \ln t$, $B = q$ when $t = 1$), R²: model fitting degree.

277

278



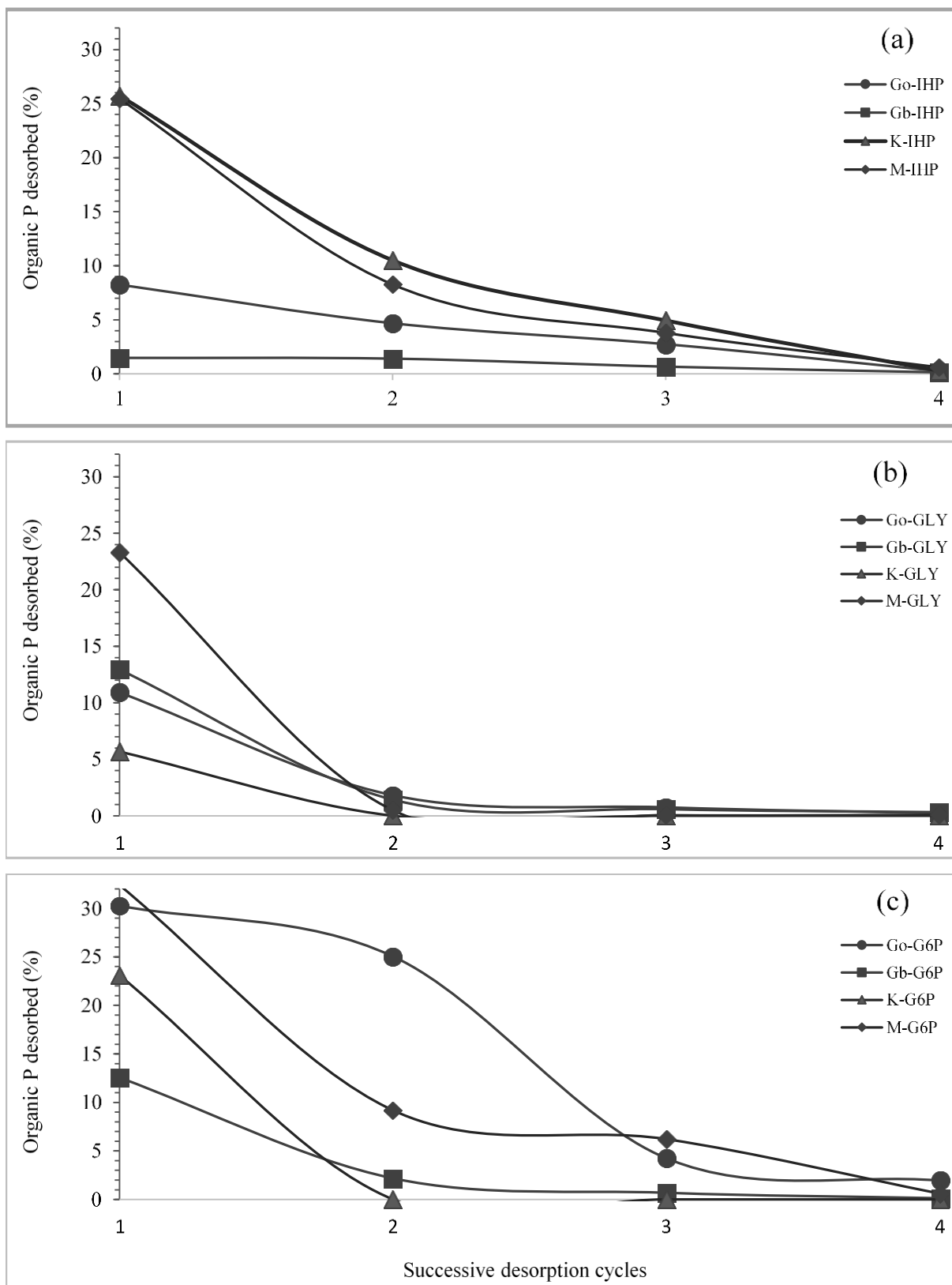
279

280 Fig. 4. Variation in P desorption rates of mineral-OP complexes.

281 3.2.2. Role of soil minerals in desorption dynamics

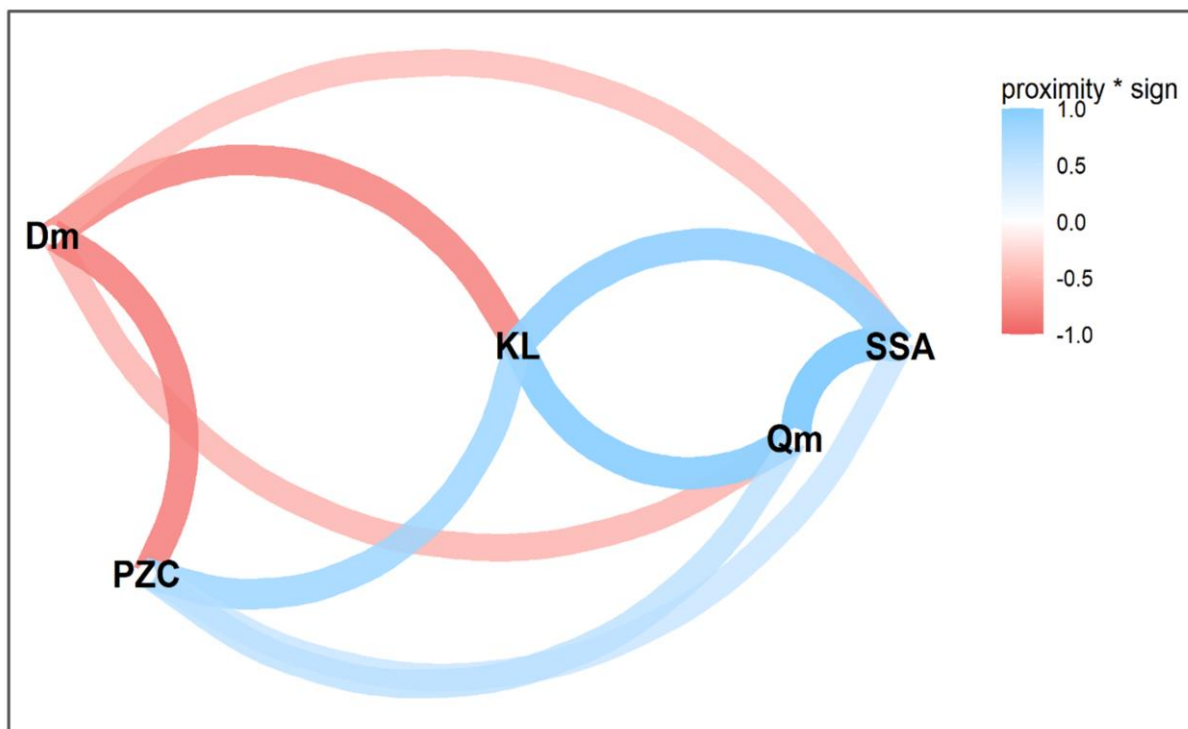
282 There was a large difference between Fe and Al oxides minerals and clays mineral with respect to
 283 desorption properties (Table 2 and Fig. 3). Phosphate desorption from Fe and Al oxides was very rapid,
 284 and equilibrium was attained within 2 days. Except for G6P on goethite, OP desorption from soil
 285 minerals at the end of the experiment could be ranked as gibbsite (3-14%) < goethite (13-14%) <
 286 kaolinite (5-39%) << montmorillonite (23-45%) (Table 2, Fig. 3). Organic P desorption from clays
 287 minerals was thus much higher than from Fe and especially Al oxides. This large difference in the
 288 capacity of soil minerals to release OP would be related to the physicochemical properties of the soil
 289 and the OP. Indeed, our results showed strong negative correlation between the desorption capacity
 290 (Dm) and the properties of the soil minerals (PZC and SSA), and the correlation appears to be stronger
 291 with PZC (Fig. 6).

292 Successive desorption (Fig. 5) using KCl showed that more than 25% of the adsorbed OP (myo-
293 IHP, G6P, GLY) on montmorillonite was desorbed in the first cycle and there was no desorption after 4
294 cycles. Compared to the clays-myo-IHP complex, P desorbed from Fe, Al oxide- myo-IHP was lower
295 but declined more slowly with increasing number of cycles (Fig. 5). The same trends were observed
296 with the Fe and Al oxide-GLY complexes. For instance, at the first cycle, more myo-IHP and GLY was
297 desorbed from the clay minerals than from the Fe and Al oxides, but from the second cycle, Fe and Al
298 oxides had desorbed almost as much myo-IHP and GLY as the clays. At the fourth cycle, the amount of
299 myo-IHP and GLY desorbed from the clay minerals was lower or equal to that from Fe and Al oxides.
300 This suggests that the clays-myo-IHP and GLY complex supplied P rapidly but over a short period
301 whereas the Fe and Al oxide-IHP and GLY complex supplied P slowly but over a long period. With
302 slight differences, the soil mineral-G6P complexes appeared to show the same trend as mineral-IHP or
303 GLY. As mentioned above for the results of the adsorption mechanisms of montmorillonite, the
304 desorption properties (kinetics, amount and rate of desorption) are also only valid for K-saturated
305 montmorillonite.



306

307 Fig. 5. Successive desorption of (a) IHP, (b) GLY and (c) G6P from OP-mineral complexes by KCl.



308

309 Fig. 6. Conceptual framework showing the linkage among soil minerals properties (PZC, SSA) and
 310 adsorption/desorption parameters (bonding strength, K_L ; adsorption capacity, Q_m , and desorption
 311 capacity, D_m). The linkage is based on the relationships between different variables. The color of each
 312 line refers to the degree of relationship between the variables. $R^2 > 0.5$

313 4. Discussion

314 4.1. Influence of organic phosphorus properties on adsorption and desorption dynamics

315 Adsorption dynamics of OP compounds play an important role in the potential reactivity of OP in soils
 316 amended with organic input. Our results showed the positive relationship between OP adsorption
 317 dynamics and the number of phosphate groups of the organic molecule. The higher phosphate group
 318 number, the higher the adsorption. Thus, myo-IHP, which has six orthophosphates per C moiety, was
 319 adsorbed in larger quantities than the orthophosphate monoesters (G6P and GLY) because it can
 320 coordinate with more hydroxyl (OH) groups on the surface of soil minerals (McKercher and Anderson,
 321 1968). The sizes of the C moiety, may be also responsible for the difference in adsorption amount of
 322 each OP compounds. Our results about molecular mass effects on OP adsorption dynamics were in

323 disagreement with most studies that found decreases in OP adsorption with increasing molecular mass
324 due to steric hindrance effects (Lü et al., 2017; Ruttenberg and Sulak, 2011). They specifically disagree
325 with those of Lü et al., (2017) who observed that the adsorption maxima of OPs on goethite and hematite
326 were classified as follows: IP > Adenosine monophosphate (AMP) = G6P > ATP, showing a decreasing
327 trend in sorption levels with increasing molecular mass of the different forms of OP. Our results also
328 contrast with those of Yan et al., (2014) where the maximum sorption densities of three Al
329 (oxyhydr)oxides (amorphous Al(OH)₃, boehmite and α-Al₂O₃) increased with decreasing molecular
330 masses follows IHP < ATP < G6P < GLY < IP. However, the results obtained agree with the work of
331 Berg and Joern, (2006), which showed a trend of increasing rather than decreasing sorption levels with
332 increasing molecular mass of different forms of OP (IHP > G6P > ATP > IP). Similarly, recent work by
333 Ganta et al., (2020) and Ahmed et al., (2021) also supported our results. They demonstrated that the
334 organic fraction of the OP may not influence the interaction of individual phosphate groups with the soil
335 and thus the effect of molecular mass steric hindrance may be insignificant.

336 After adsorption, the ability of OP compounds to desorb depends not only on their chemical
337 properties but also on the degree of energy with which they are adsorbed onto soil minerals (Ganta et
338 al., 2021, 2019). A general weaker or equal binding strength of myo-IHP compared to GLY or G6P was
339 found. This disagrees with recent results that reported total interaction energies (in absolute value)
340 measured for goethite-IHP complexes (-72 to -85 kcal mol⁻¹) higher than those for GLY (-38 to -48 kcal
341 mol⁻¹) (Ganta et al., 2019; Kubicki et al., 2012; Rakovan et al., 1999). In addition, this finding also
342 contradicts the extensive literature that associates the large amount of IHP adsorbed with its strong
343 binding to minerals (Celi et al., 2000; Giaveno et al., 2008; Guan et al., 2006; Johnson et al., 2012; Xu
344 et al., 2017). However, this indicates that the higher adsorption of IHP relative to other OP compounds
345 did not necessarily imply that its binding capacity is always strong and stable under all environmental
346 conditions. Thus, we suggest that despite the higher accumulation of myo-IHP reported in most soils
347 (Amadou et al., 2021; Gerke, 2015), its desorption may be easier than that of the GLY or G6P forms,
348 although this depends greatly on the soil minerals and experimental conditions. Furthermore, our results
349 indicated that if both GLY and G6P species compete with myo-IHP for the same active sites on soil
350 minerals, the binding energy of GLY or G6P would be higher than that of myo-IHP. Therefore, one

351 could expect easier desorption of myo-IHP from soil compared to GLY and G6P even though this would
352 be highly dependent on soil minerals.

353 4.2. Influence of soil mineral characteristics on adsorption and desorption dynamics

354 The tested soil minerals presented a different capacity to sorb OP compounds due to their contrasting
355 physicochemical properties. Fe and Al oxides showed very different OP adsorption mechanisms
356 compared to clays, as the adsorption capacity ranked as follows: kaolinite < montmorillonite < goethite
357 <<< gibbsite. This can be explained by their contrasting types of surface charge. At pH 5.5 (pH used for
358 this study), kaolinite has a small net negative charge, goethite has a small net positive charge and gibbsite
359 is positively charged while montmorillonite is negatively charged according to their PZC values (He et
360 al., 1994; He and Zhu, 1997). Gibbsite exhibited the greatest adsorption maximum, which was probably
361 related to the combined effect of its high surface positive charge and greater SSA (120-364 m² g⁻¹), as
362 well as the abundance of active adsorption sites, as noted by Shang et al., (1990) and Yan et al., (2014).
363 Manning and Goldberg, (1996) found that gibbsite and goethite adsorbed roughly 23 times more P than
364 kaolinite and up to 53.5 times more IP than montmorillonite and illite. However, despite the highest OP
365 adsorption capacity of gibbsite, its interaction energy with OP would be less strong than IP. The order
366 of the K_L value, i.e., binding energy (clays << Fe and Al oxides), suggests a much higher binding energy
367 between OP and Fe and Al oxides than between OP and clays. These results suggest that the mechanism
368 of OP adsorption on Fe and Al oxides is quite different from that on clay minerals. In sum, soil minerals
369 had diverse adsorption mechanisms, specifically Fe and Al oxides compared to clay minerals. The
370 changes in their adsorption and binding capacity to OP compounds were the result of their contrasting
371 physicochemical properties. This may result in different behavior in the desorption of adsorbed Po.
372 However, since it is well known that the number of positive charges of variably charged minerals
373 (especially Fe and Al oxyhydroxides and kaolinite) decreases with increasing pH, we speculate that their
374 adsorption may decrease at higher pH than that of our study (i.e. pH > 5.5)(Hu et al., 2020b). In addition,
375 it is also known that cations in solution can affect the P sorption potential of certain minerals, e.g., Al
376 or Ca saturated clay minerals (Ellis Jr and Truog, 1955; Pissarides et al., 1968; Prietzel et al., 2016). The

377 next challenge will be therefore to elucidate the role various cations on OP retention by minerals. This
378 could also allow to feed surface complexation models to gain in robustness on the understanding of the
379 adsorption and desorption mechanisms while better predicting P behavior in soils.

380 The desorption dynamics of the adsorbed OP was markedly affected by both OP and soil
381 minerals characteristics. OP was more desorbed from clays minerals (montmorillonite and kaolinite)
382 than from Fe and Al oxides. Since clays have also been shown to have a lower OP retention capacity, it
383 can be expected that OP will be more available when organic inputs are applied to soils dominated by
384 phyllosilicates, e.g. subtropical and temperate soils (Bortoluzzi et al., 2015; He et al., 1994).
385 Furthermore, with time, OP desorption kinetics and rate differed between soil minerals. Our findings
386 showed that clays-OP complex released P rapidly but over a short period whereas the Fe and Al oxide-
387 OP complex released slowly but over a longer period. In the clay-OP complexes, the binding energy
388 would be unstable and its distribution would have varied remarkably with time, probably from loosely-
389 bound fraction to tightly-bound fraction. In contrasts, Fe and Al oxide-OP complexes were stable with
390 time. These results indicated that each complex would have presented a different binding mechanism,
391 e.g. the inner sphere versus the outer sphere complex with different types of bonds e.g. bidentate versus
392 monodentate (Ganta et al., 2019). Our results highlighted the central role of OPs and their interactions
393 with soil minerals on P availability and potential P loss to water. Better knowledge of these interactions
394 constitutes an important challenge to model OP dynamics and predict P release to plants and waters in
395 soil amended with OP fertilizers. Despite the overall low desorption of OP from Fe and Al complexes,
396 G6P and GLY were however more desorbed from goethite and gibbsite than IP. This weaker retention
397 of these OP forms by Fe and Al oxides suggests that both G6P and GLY could be used in Fe/Al oxide-
398 rich soils to improve P nutrition of plants. This has therefore great implication for P fertilization in
399 highly weathered soils of tropical regions in which Fe and/or Al oxides are dominant. Taken together,
400 our results indicate that both Fe and Al oxides and clay minerals in soil could be either OP sinks or OP
401 sources, depending on their properties, binding energy and adsorption saturation.

402 It must be noted, however, that soils may contain a much wider variety of Fe and Al oxides
403 than those used in this study, namely goethite and gibbsite respectively. For example, many soils contain
404 significant amounts of ferrihydrite, which was reported to have a higher P sorption than goethite

405 (Prietz et al., 2016; Ruttens and Sulak, 2011; Prietz and Klysubun, 2018). As an outlook, we
406 strongly suggest studies to better understand the involvement of a wide range of iron oxides in the
407 dynamics of OP forms. More generally, though our results provide a mechanistic understanding of the
408 sorption processes of various OP forms on selected soil minerals, the role of other soil minerals alone
409 or in combination needs still to be investigated to generate a better overview of OP dynamics in real
410 complex soil systems. In addition, it is also important to point out that our results regarding the
411 comparison between the P (de)sorption properties of montmorillonite and other soil minerals are only
412 valid for the K-saturated montmorillonite used here. For Al- or Ca-saturated montmorillonite, a much
413 stronger P sorption or less pronounced P desorption would be expected compared to K-saturated
414 montmorillonite. Furthermore, in agroecosystems, with the exception of periods immediately following
415 heavy K fertilization, K-saturated montmorillonite, which was used here as the montmorillonite type, is
416 rare in most soils. Thus, the results must be considered in light of the type of clay used (K-saturated
417 montmorillonite in this study).

418 4.3. Adsorption and desorption dynamics of OP relative to IP

419 Compared to IP, myo-IHP was generally more strongly adsorbed whereas the opposite was observed
420 for G6P and GLY. This result showed that specific forms of OP, depending on their characteristics, had
421 contrasting adsorption dynamics with respect to IP. Therefore, the weaker retention of OP compared to
422 IP which is generally suggested in the literature (Anderson et al., 1974; Condon et al., 2015, 2005) did
423 not apply to all organic P compounds as higher inositol phosphate esters can be strongly retained in soil.
424 Berg and Joern, (2006) found that soils pretreated with myo-IHP or having combinations of myo-IHP
425 and IP in solution had reduced IP adsorption by successfully competing for binding sites, indicating that
426 there was a preference in the adsorption of myo-IHP over IP. This preference may either lead to the
427 release of already adsorbed IP or prevent further adsorption of IP, leading to an increase in both available
428 IP for plants and soluble IP for runoff (Leytem et al., 2002). Furthermore, in the presence of different
429 OP forms in soils, the preferential adsorption of myo-IHP or IP over both G6P and GLY may increase
430 G6P and GLY availability and promote their mineralization. Thus, this contrasting adsorption dynamics
431 of OP versus IP have important implications for P management from organic input in soils because IHP,

432 GLY and G6P can comprise up to 80% of total P in some organic input (Amadou et al., 2021; Darch et
433 al., 2014; George et al., 2018), and many animal manures, notably those from monogastrics (pigs,
434 poultry), contain substantial quantities of inositol phosphates (Hu et al., 2020a; Peperzak et al., 1959).
435 Application of these manures to agricultural land could, therefore, promote the solubilization of IP
436 and/or reduce the adsorption of G6P and GLY which would then be available for uptake by plants but
437 also released into runoff water (Reid et al., 2018). On most soil minerals, the amount of desorbed OP
438 and the desorbed rate of OP were generally lower than those of IP. After several desorption cycles, (Roy
439 et al., 2017) found that 20% of IP desorbed from goethite while it only accounted for less than 5% for
440 OP. Similar findings were reported by (Ruyter-Hooley et al., 2016) with limited desorption of OP (<3%
441 of total amount) on gibbsite, even in the presence of humic acids as competing ligands for sorption sites.
442 Huang and Zhang, (2012) showed that OP compounds added by organic input may desorb slowly and
443 mineralized in step with plant uptake, even in the long term. However, our results showed that this did
444 not apply to all OP compounds.

445 **5. Concluding remarks**

446 Moving toward more sustainable sources for managing P nutrition in agroecosystems, OP derived from
447 organic inputs and soil is increasingly considered to complement mineral P fertilizer. However,
448 enhancing OP cycling and availability in soils while reducing OP loss into the environment requires a
449 better understanding of OP adsorption/desorption processes on soil minerals. Factors related to soil
450 properties and OP molecular characteristics directly affect the reactions of OP and its release into the
451 soil. The myo-IHP, GLY and G6P form showed different adsorption processes from each other as well
452 as from the IP form. Our results demonstrated contrasted adsorption capacities between myo-IHP and
453 the other organic P forms (G6P and GLY) relative to IP form, with myo-IHP exhibiting the greatest
454 adsorption capacities. The adsorption capacity of each OP compounds is determined by the number of
455 orthophosphate groups associated with the C moiety in each compound and its size. The general idea of
456 a lower adsorption of OP relative to IP suggested by the literature does not match for all OP compounds
457 since, even though myo-IHP was more strongly retained relative to IP, G6P and GLY were more weakly
458 retained. In general, OP compounds showed less desorption and slower desorption rate per day than IP

459 forms. Fe and Al oxides showed very different OP adsorption mechanisms compared to clays regarding
460 their binding energy and adsorption amount, which were related to different in properties (SSA and
461 PZC). The Fe and especially Al oxides (gibbsite) exhibited the highest maximum adsorption capacity
462 for all OP forms.

463 The desorption dynamics of the adsorbed OP was markedly affected by both OP and soil
464 minerals characteristics. Montmorillonite showed the highest desorption for OP suggesting higher OP
465 release when organic inputs are applied soils dominated by 2:1 phyllosilicate. However, the results are
466 very dependent on the specific type of montmorillonite used in this study. In fact, the results related to
467 the comparison between the P (de)sorption properties of montmorillonite and other soil minerals are
468 only valid for the K-saturated montmorillonite used here. If Al- or Ca-saturated montmorillonite, which
469 are the most common types of montmorillonite in soils, had been used, much higher P sorption and
470 lower P desorption would be expected compared to K-saturated montmorillonite. Finally, despite their
471 overall high adsorption, the higher desorption of G6P or GLY relative to IP from Fe and Al oxides
472 indicated that G6P and GLY release would be less affected than IP by such soil compounds, which are
473 especially abundant in highly weathered soils. However, since the P concentration used in our study
474 may be higher than that of real soil systems, it would be interesting to investigate the effect of P
475 concentration on adsorption processes by performing sorption experiments at different (and lower) P
476 concentrations.

477 By simultaneously analyzing the interactions between various OP forms and various soil
478 minerals, this study provides new insight into the OP adsorption and desorption dynamics on soil
479 minerals which is important to optimize the use of organic input as fertilizer and to improve or develop
480 prediction model of OP release in agroecosystems.

481 **Declaration of Competing Interest**

482 The authors declare that they have no known competing financial interests or personal relationships that
483 could have appeared to influence the work reported in this paper.

484 **Acknowledgements**

485 Acknowledgments: The authors thank the Institut Polytechnique UniLaSalle Beauvais and Pro-gramme
486 Opérationnel FEDER/FSE Picardie 2014–2020 for their support for the start of the global research
487 project in agriculture focusing on sustainable management of soil fertility and ecoefficiency of
488 phosphorus management in farming systems. We also thank Adaline Adam, Céline Roisin, Aurore
489 Coutelier, Nicolas HONVAULT, Philippe Jacolot, Hamza MOHIEDDINNE for their technical
490 assistance.

491 **References**

- 492 Ahmed, W., Jing, H., Kailou, L., Ali, S., Tianfu, H., Geng, S., Jin, C., Qaswar, M., Jiangxue,
493 D., Mahmood, S., Maitlo, A.A., Khan, Z.H., Zhang, H., Chen, D.-Y., 2021. Impacts of
494 long-term inorganic and organic fertilization on phosphorus adsorption and desorption
495 characteristics in red paddies in southern China. PLOS ONE 16, e0246428.
496 <https://doi.org/10.1371/journal.pone.0246428>
- 497 Amadou, I., Houben, D., Faucon, M.-P., 2021. Unravelling the Role of Rhizosphere
498 Microbiome and Root Traits in Organic Phosphorus Mobilization for Sustainable
499 Phosphorus Fertilization. A Review. Agronomy 11, 2267.
500 <https://doi.org/10.3390/agronomy11112267>
- 501 Anderson, G., Arlidge, E.Z., 1962. The adsorption of inositol phosphates and glycerophosphate
502 by soil clays, clay minerals, and hydrated sesquioxides in acid media. Journal of Soil
503 Science 13, 216–224. <https://doi.org/10.1111/j.1365-2389.1962.tb00699.x>
- 504 Anderson, G., Williams, E.G., Moir, J.O., 1974. A Comparison of the Sorption of Inorganic
505 Orthophosphate and Inositol Hexaphosphate by Six Acid Soils. Journal of Soil Science
506 25, 51–62. <https://doi.org/10.1111/j.1365-2389.1974.tb01102.x>
- 507 Andrino, A., Boy, J., Mikutta, R., Sauheitl, L., Guggenberger, G., 2019. Carbon Investment
508 Required for the Mobilization of Inorganic and Organic Phosphorus Bound to Goethite
509 by an Arbuscular Mycorrhiza (*Solanum lycopersicum* x *Rhizophagus irregularis*).
510 Frontiers in Environmental Science 7 (2019), Nr. 26 7. <https://doi.org/10.15488/4844>
- 511 Archontoulis, S.V., Miguez, F.E., 2015. Nonlinear Regression Models and Applications in
512 Agricultural Research. Agronomy Journal 107, 786–798.
513 <https://doi.org/10.2134/agronj2012.0506>
- 514 Barrow, N.J., 1986. Reaction of Anions and Cations with Variable-Charge Soils, in: Advances
515 in Agronomy. Elsevier, pp. 183–230. [https://doi.org/10.1016/S0065-2113\(08\)60676-8](https://doi.org/10.1016/S0065-2113(08)60676-8)
- 516 Bates, D., Watts, D.G., 1988. Nonlinear Regression Analysis and Its Applications.
517 <https://doi.org/10.2307/1268866>

- 518 Berg, A.S., Joern, B.C., 2006. Sorption Dynamics of Organic and Inorganic Phosphorus
519 Compounds in Soil. *J. Environ. Qual.* 35, 1855–1862.
520 <https://doi.org/10.2134/jeq2005.0420>
- 521 Bollyn, J., Faes, J., Fritzsche, A., Smolders, E., 2017. Colloidal-Bound Polyphosphates and
522 Organic Phosphates Are Bioavailable: A Nutrient Solution Study. *J. Agric. Food Chem.*
523 65, 6762–6770. <https://doi.org/10.1021/acs.jafc.7b01483>
- 524 Bortoluzzi, E.C., Pérez, C.A.S., Ardisson, J.D., Tiecher, T., Caner, L., 2015. Occurrence of iron
525 and aluminum sesquioxides and their implications for the P sorption in subtropical soils.
526 *Applied Clay Science* 104, 196–204. <https://doi.org/10.1016/j.clay.2014.11.032>
- 527 Brown, A.M., 2001. A step-by-step guide to non-linear regression analysis of experimental data
528 using a Microsoft Excel spreadsheet. *Computer Methods and Programs in Biomedicine*
529 65, 191–200. [https://doi.org/10.1016/S0169-2607\(00\)00124-3](https://doi.org/10.1016/S0169-2607(00)00124-3)
- 530 Bulut, E., Özacar, M., Şengil, İ.A., 2008. Adsorption of malachite green onto bentonite:
531 equilibrium and kinetic studies and process design. *Microporous and mesoporous*
532 *materials* 115, 234–246.
- 533 Celi, L., Lamacchia, S., Barberis, E., 2000. Interaction of inositol phosphate with calcite.
534 *Nutrient Cycling in Agroecosystems* 57, 271–277.
535 <https://doi.org/10.1023/A:1009805501082>
- 536 Celi, L., Lamacchia, S., Marsan, F.A., Barberis, E., 1999. Interaction of inositol hexaphosphate
537 on clays: adsorption and charging phenomena: *soil science* 164, 574–585.
538 <https://doi.org/10.1097/00010694-199908000-00005>
- 539 Condon, L.M., Turner, B.L., Cade-Menun, B.J., 2015. Chemistry and Dynamics of Soil
540 Organic Phosphorus, in: Thomas Sims, J., Sharpley, A.N. (Eds.), *Agronomy*
541 *Monographs*. American Society of Agronomy, Crop Science Society of America, and
542 *Soil Science Society of America*, Madison, WI, USA, pp. 87–121.
543 <https://doi.org/10.2134/agronmonogr46.c4>
- 544 Condon, L.M., Turner, B.L., Cade-Menun, B.J., 2005. Chemistry and Dynamics of Soil
545 Organic Phosphorus, in: *Phosphorus: Agriculture and the Environment*. John Wiley &
546 *Sons, Ltd*, pp. 87–121. <https://doi.org/10.2134/agronmonogr46.c4>
- 547 Crini, G., Peindy, H.N., Gimbert, F., Robert, C., 2007. Removal of C.I. Basic Green 4
548 (Malachite Green) from aqueous solutions by adsorption using cyclodextrin-based
549 adsorbent: Kinetic and equilibrium studies. *Separation and Purification Technology* 53,
550 97–110. <https://doi.org/10.1016/j.seppur.2006.06.018>
- 551 Darch, T., Blackwell, M.S.A., Hawkins, J.M.B., Haygarth, P.M., Chadwick, D., 2014. A Meta-
552 Analysis of Organic and Inorganic Phosphorus in Organic Fertilizers, Soils, and Water:
553 Implications for Water Quality. *Critical Reviews in Environmental Science and*
554 *Technology* 44, 2172–2202. <https://doi.org/10.1080/10643389.2013.790752>
- 555 Deiss, L., de Moraes, A., Maire, V., 2018. Environmental drivers of soil phosphorus
556 composition in natural ecosystems. *Biogeosciences* 15, 4575–4592.
557 <https://doi.org/10.5194/bg-15-4575-2018>

- 558 Doolette, A.L., Smernik, R.J., Dougherty, W.J., 2011. A quantitative assessment of phosphorus
559 forms in some Australian soils. *Soil Research* 49, 152–165.
- 560 Ellis Jr, R., Truog, E., 1955. Phosphate fixation by montmorillonite. *Soil Science Society of*
561 *America Journal* 19, 451–454.
- 562 Faucon, M.-P., Houben, D., Reynoird, J.-P., Mercadal-Dulaurent, A.-M., Armand, R., Lambers,
563 H., 2015. Advances and Perspectives to Improve the Phosphorus Availability in
564 Cropping Systems for Agroecological Phosphorus Management, in: *Advances in*
565 *Agronomy*. Elsevier, pp. 51–79. <https://doi.org/10.1016/bs.agron.2015.06.003>
- 566 Fuentes, B., Bolan, N., Naidu, R., Mora, M. de la L., 2006. Phosphorus in organic waste-soil
567 systems. *R.C. Suelo Nutr. Veg.* 6. <https://doi.org/10.4067/S0718-27912006000200006>
- 568 Ganta, P.B., Kühn, O., Ahmed, A.A., 2020. QM/MM molecular dynamics investigation of the
569 binding of organic phosphates to the 100 diaspore surface.
- 570 Ganta, P.B., Kühn, O., Ahmed, A.A., 2019. QM/MM simulations of organic phosphorus
571 adsorption at the diaspore–water interface. *Phys. Chem. Chem. Phys.* 21, 24316–24325.
572 <https://doi.org/10.1039/C9CP04032C>
- 573 Ganta, P.B., Morshedizad, M., Kühn, O., Leinweber, P., Ahmed, A.A., 2021. The Binding of
574 Phosphorus Species at Goethite: A Joint Experimental and Theoretical Study (preprint).
575 CHEMISTRY. <https://doi.org/10.20944/preprints202102.0171.v1>
- 576 George, T.S., Giles, C.D., Menezes-Blackburn, D., Condron, L.M., Gama-Rodrigues, A.C.,
577 Jaisi, D., Lang, F., Neal, A.L., Stutter, M.I., Almeida, D.S., Bol, R., Cabugao, K.G.,
578 Celi, L., Cotner, J.B., Feng, G., Goll, D.S., Hallama, M., Krueger, J., Plassard, C.,
579 Rosling, A., Darch, T., Fraser, T., Giesler, R., Richardson, A.E., Tamburini, F., Shand,
580 C.A., Lumsdon, D.G., Zhang, H., Blackwell, M.S.A., Wearing, C., Mezeli, M.M.,
581 Almås, Å.R., Audette, Y., Bertrand, I., Beyhaut, E., Boitt, G., Bradshaw, N., Brearley,
582 C.A., Bruulsema, T.W., Ciais, P., Cozzolino, V., Duran, P.C., Mora, M.L., de Menezes,
583 A.B., Dodd, R.J., Dunfield, K., Engl, C., Frazão, J.J., Garland, G., González Jiménez,
584 J.L., Graca, J., Granger, S.J., Harrison, A.F., Heuck, C., Hou, E.Q., Johnes, P.J., Kaiser,
585 K., Kjær, H.A., Klumpp, E., Lamb, A.L., Macintosh, K.A., Mackay, E.B., McGrath, J.,
586 McIntyre, C., McLaren, T., Mészáros, E., Missong, A., Mooshammer, M., Negrón, C.P.,
587 Nelson, L.A., Pfahler, V., Poblete-Grant, P., Randall, M., Seguel, A., Seth, K., Smith,
588 A.C., Smits, M.M., Sobarzo, J.A., Spohn, M., Tawaraya, K., Tibbett, M., Voroney, P.,
589 Wallander, H., Wang, L., Wasaki, J., Haygarth, P.M., 2018. Organic phosphorus in the
590 terrestrial environment: a perspective on the state of the art and future priorities. *Plant*
591 *Soil* 427, 191–208. <https://doi.org/10.1007/s11104-017-3391-x>
- 592 Gerke, J., 2015. Phytate (Inositol Hexakisphosphate) in Soil and Phosphate Acquisition from
593 Inositol Phosphates by Higher Plants. A Review. *Plants* 4, 253–266.
594 <https://doi.org/10.3390/plants4020253>
- 595 Giaveno, C., Celi, L., Cessa, R.M.A., Prati, M., Bonifacio, E., Barberis, E., 2008. Interaction
596 of organic phosphorus with clays extracted from oxisols. *Soil Science* 173, 694–706.
597 <https://doi.org/10.1097/SS.0b013e3181893b59>

- 598 Giles, C., Cade-Menun, B., Hill, J., 2011. The inositol phosphates in soils and manures:
599 Abundance, cycling, and measurement. *Can. J. Soil. Sci.* 91, 397–416.
600 <https://doi.org/10.4141/cjss09090>
- 601 Goebel, M.-O., Adams, F., Boy, J., Guggenberger, G., Mikutta, R., 2017. Mobilization of
602 glucose-6-phosphate from ferrihydrite by ligand-promoted dissolution is higher than of
603 orthophosphate. *J. Plant Nutr. Soil Sci.* 180, 279–282.
604 <https://doi.org/10.1002/jpln.201600479>
- 605 Guan, X.-H., Shang, C., Zhu, J., Chen, G.-H., 2006. ATR-FTIR investigation on the
606 complexation of myo-inositol hexaphosphate with aluminum hydroxide. *Journal of*
607 *Colloid and Interface Science* 293, 296–302. <https://doi.org/10.1016/j.jcis.2005.06.070>
- 608 Guzman, G., Alcantara, E., Barron, V., Torrent, J., 1994. Phytoavailability of phosphate
609 adsorbed on ferrihydrite, hematite, and goethite. *Plant Soil* 159, 219–225.
610 <https://doi.org/10.1007/BF00009284>
- 611 Hansen, N.C., Daniel, T.C., Sharpley, A.N., Lemunyon, J.L., 2002. The fate and transport of
612 phosphorus in agricultural systems. *Journal of Soil and Water Conservation* 57, 408–
613 417.
- 614 He, Z.L., Yang, X., Yuan, K.N., Zhu, Z.X., 1994. Desorption and plant-availability of
615 phosphate sorbed by some important minerals. *Plant Soil* 162, 89–97.
616 <https://doi.org/10.1007/BF01416093>
- 617 He, Z.L., Zhu, J., 1997. Transformation and bioavailability of specifically sorbed phosphate on
618 variable-charge minerals in soils. *Biology and Fertility of Soils* 25, 175–181.
619 <https://doi.org/10.1007/s003740050300>
- 620 Houben, D., Meunier, C., Pereira, B., Sonnet, Ph., 2011. Predicting the degree of phosphorus
621 saturation using the ammonium acetate-EDTA soil test: Degree of phosphorus
622 saturation in soils. *Soil Use and Management* no-no. <https://doi.org/10.1111/j.1475-2743.2011.00353.x>
- 624 Hu, Z., Jaisi, D.P., Yan, Y., Chen, H., Wang, X., Wan, B., Liu, F., Tan, W., Huang, Q., Feng,
625 X., 2020a. Adsorption and precipitation of *myo*-inositol hexakisphosphate onto
626 kaolinite. *Eur J Soil Sci* 71, 226–235. <https://doi.org/10.1111/ejss.12849>
- 627 Hu, Z., Jaisi, D.P., Yan, Y., Chen, H., Wang, X., Wan, B., Liu, F., Tan, W., Huang, Q., Feng,
628 X., 2020b. Adsorption and precipitation of *myo*-inositol hexakisphosphate onto
629 kaolinite. *European Journal of Soil Science* 71, 226–235.
- 630 Huang, X.-L., Zhang, J.-Z., 2012. Hydrolysis of glucose-6-phosphate in aged, acid-forced
631 hydrolysed nanomolar inorganic iron solutions—an inorganic biocatalyst? *RSC Adv.* 2,
632 199–208. <https://doi.org/10.1039/C1RA00353D>
- 633 Johnson, B.B., Quill, E., Angove, M.J., 2012. An investigation of the mode of sorption of
634 inositol hexaphosphate to goethite. *Journal of Colloid and Interface Science* 367, 436–
635 442. <https://doi.org/10.1016/j.jcis.2011.09.066>

- 636 Kahiluoto, H., Kuisma, M., Ketoja, E., Salo, T., Heikkinen, J., 2015. Phosphorus in Manure
637 and Sewage Sludge More Recyclable than in Soluble Inorganic Fertilizer. *Environ. Sci.*
638 *Technol.* 49, 2115–2122. <https://doi.org/10.1021/es503387y>
- 639 Khare, N., Hesterberg, D., Beauchemin, S., Wang, S.-L., 2004. XANES Determination of
640 Adsorbed Phosphate Distribution between Ferrihydrite and Boehmite in Mixtures. *Soil*
641 *Sci. Soc. Am. J.* 68, 460–469. <https://doi.org/10.2136/sssaj2004.4600>
- 642 Kubicki, J.D., Paul, K.W., Kabalan, L., Zhu, Q., Mroziak, M.K., Aryanpour, M., Pierre-Louis,
643 A.-M., Strongin, D.R., 2012. ATR–FTIR and Density Functional Theory Study of the
644 Structures, Energetics, and Vibrational Spectra of Phosphate Adsorbed onto Goethite.
645 *Langmuir* 28, 14573–14587. <https://doi.org/10.1021/la303111a>
- 646 Lagos, L.M., Acuña, J.J., Maruyama, F., Ogram, A., de la Luz Mora, M., Jorquera, M.A., 2016.
647 Effect of phosphorus addition on total and alkaline phosphomonoesterase-harboring
648 bacterial populations in ryegrass rhizosphere microsites. *Biol Fertil Soils* 52, 1007–
649 1019. <https://doi.org/10.1007/s00374-016-1137-1>
- 650 Langmuir, I., 1918. The adsorption of gases on plane surfaces of glass, mica and platinum. *J.*
651 *Am. Chem. Soc.* 40, 1361–1403. <https://doi.org/10.1021/ja02242a004>
- 652 Leytem, A.B., Mikkelsen, R.L., Gilliam, J.W., 2002. Sorption of organic phosphorus
653 compounds in atlantic coastal plain soils: *Soil Science* 167, 652–658.
654 <https://doi.org/10.1097/00010694-200210000-00003>
- 655 Lü, C., Yan, D., He, J., Zhou, B., Li, L., Zheng, Q., 2017. Environmental geochemistry
656 significance of organic phosphorus: An insight from its adsorption on iron oxides.
657 *Applied Geochemistry* 84, 52–60. <https://doi.org/10.1016/j.apgeochem.2017.05.026>
- 658 Manning, B.A., Goldberg, S., 1996. Modeling arsenate competitive adsorption on kaolinite,
659 montmorillonite and illite. *Clays and Clay Minerals* 44, 609–623.
660 <https://doi.org/10.1346/CCMN.1996.0440504>
- 661 Manning, Bruce A., Goldberg, S., 1996. Modeling Competitive Adsorption of Arsenate with
662 Phosphate and Molybdate on Oxide Minerals. *Soil Science Society of America Journal*
663 60, 121–131. <https://doi.org/10.2136/sssaj1996.03615995006000010020x>
- 664 McKercher, R.B., Anderson, G., 1968. Characterization of the inositol penta-and
665 hexaphosphate fractions of a number of Canadian and Scottish soils. *Journal of Soil*
666 *Science* 19, 302–310.
- 667 Monbet, P., McKelvie, I.D., Worsfold, P.J., 2009. Dissolved organic phosphorus speciation in
668 the waters of the Tamar estuary (SW England). *Geochimica et Cosmochimica Acta* 73,
669 1027–1038. <https://doi.org/10.1016/j.gca.2008.11.024>
- 670 Nair, P.S., Logan, T.J., Sharpley, A.N., Sommers, L.E., Tabatabai, M.A., Yuan, T.L., 1984.
671 Interlaboratory Comparison of a Standardized Phosphorus Adsorption Procedure. *J.*
672 *environ. qual.* 13, 591–595. <https://doi.org/10.2134/jeq1984.00472425001300040016x>
- 673 Newman, R.H., Tate, K.R., 1980. Soil phosphorus characterisation by ³¹P nuclear magnetic
674 resonance. *Communications in Soil Science and Plant Analysis* 11, 835–842.

- 675 Ohno, T., Zibilske, L.M., 1991. Determination of Low Concentrations of Phosphorus in Soil
676 Extracts Using Malachite Green. *Soil Science Society of America Journal* 55, 892–895.
677 <https://doi.org/10.2136/sssaj1991.03615995005500030046x>
- 678 Parfitt, R.L., 1979. The availability of P from phosphate-goethite bridging complexes.
679 Desorption and uptake by ryegrass. *Plant Soil* 53, 55–65.
680 <https://doi.org/10.1007/BF02181879>
- 681 Peperzak, P., Caldwell, A.G., Hunziker, R.R., Black, C.A., 1959. Phosphorus fractions in
682 manures. *Soil Science* 87, 293–302.
- 683 Peters, J.P., Van Slyke, D.D., 1932. *Quantitative clinical chemistry: J.P. Peters and D.D. Van*
684 *Slyke*. Williams & Wilkins, Baltimore.
- 685 Pissarides, A., Stewart, J.W.B., Rennie, D.A., 1968. Influence of cation saturation on
686 phosphorus adsorption by selected clay minerals. *Canadian Journal of Soil Science* 48,
687 151–157.
- 688 Prietzel, J., Harrington, G., Häusler, W., Heister, K., Werner, F., Klysubun, W., 2016.
689 Reference spectra of important adsorbed organic and inorganic phosphate binding forms
690 for soil P speciation using synchrotron-based K -edge XANES spectroscopy. *J*
691 *Synchrotron Rad* 23, 532–544. <https://doi.org/10.1107/S1600577515023085>
- 692 Prietzel, J., Klysubun, W., 2018. Phosphorus K -edge XANES spectroscopy has probably often
693 underestimated iron oxyhydroxide-bound P in soils. *J Synchrotron Rad* 25, 1736–1744.
694 <https://doi.org/10.1107/S1600577518013334>
- 695 Rakovan, J., Becker, U., Hochella, M.F., 1999. Aspects of goethite surface microtopography,
696 structure, chemistry, and reactivity. *American Mineralogist* 84, 884–894.
697 <https://doi.org/10.2138/am-1999-5-623>
- 698 Reid, K., Schneider, K., McConkey, B., 2018. Components of phosphorus loss from
699 agricultural landscapes, and how to incorporate them into risk assessment tools.
700 *Frontiers in Earth Science* 6, 135.
- 701 Roy, E.D., Willig, E., Richards, P.D., Martinelli, L.A., Vazquez, F.F., Pegorini, L., Spera, S.A.,
702 Porder, S., 2017. Soil phosphorus sorption capacity after three decades of intensive
703 fertilization in Mato Grosso, Brazil. *Agriculture, Ecosystems & Environment* 249, 206–
704 214. <https://doi.org/10.1016/j.agee.2017.08.004>
- 705 Ruttenberg, K.C., Sulak, D.J., 2011. Sorption and desorption of dissolved organic phosphorus
706 onto iron (oxyhydr)oxides in seawater. *Geochimica et Cosmochimica Acta* 75, 4095–
707 4112. <https://doi.org/10.1016/j.gca.2010.10.033>
- 708 Ruyter-Hooley, M., Morton, D.W., Johnson, B.B., Angove, M.J., 2016. The effect of humic
709 acid on the sorption and desorption of myo-inositol hexaphosphate to gibbsite and
710 kaolinite: Humic acid affects phytic acid sorption. *Eur J Soil Sci* 67, 285–293.
711 <https://doi.org/10.1111/ejss.12335>
- 712 Shang, C., Huang, P.M., Stewart, J.W.B., 1990. Kinetics of adsorption of organic and inorganic
713 phosphates by short-range ordered precipitate of aluminum. *Can. J. Soil. Sci.* 70, 461–
714 470. <https://doi.org/10.4141/cjss90-045>

- 715 Sharpley, A.N., McDowell, R.W., Kleinman, P.J., 2001. Phosphorus loss from land to water:
716 integrating agricultural and environmental management. *Plant and soil* 237, 287–307.
- 717 Tisdale, S.L., Nelson, W.L., 1966. *Soil Fertility and Fertilizers*. *Soil Science* 101, 346.
- 718 Turner, B.L., Papházy, M.J., Haygarth, P.M., Mckelvie, I.D., 2002. Inositol phosphates in the
719 environment. *Phil. Trans. R. Soc. Lond. B* 357, 449–469.
720 <https://doi.org/10.1098/rstb.2001.0837>
- 721 Urrutia, O., Guardado, I., Erro, J., Mandado, M., García-Mina, J.M., 2013. Theoretical chemical
722 characterization of phosphate-metal–humic complexes and relationships with their
723 effects on both phosphorus soil fixation and phosphorus availability for plants. *Journal*
724 *of the Science of Food and Agriculture* 93, 293–303.
- 725 Vincent, A.G., Vestergren, J., Grobner, G., Persson, P., Schleucher, J., Giesler, R., 2013. Soil
726 organic phosphorus transformations in a boreal forest chronosequence. *Plant & Soil*
727 367, 149–162. <https://doi.org/10.1007/s11104-013-1731-z>
- 728 Xu, C.-Y., Li, J.-Y., Xu, R.-K., Hong, Z.-N., 2017. Sorption of organic phosphates and its
729 effects on aggregation of hematite nanoparticles in monovalent and bivalent solutions.
730 *Environ Sci Pollut Res Int* 24, 7197–7207. <https://doi.org/10.1007/s11356-017-8382-1>
- 731 Yan, Y.P., Liu, F., Li, W., Liu, F., Feng, X.H., Sparks, D.L., 2014. Sorption and desorption
732 characteristics of organic phosphates of different structures on aluminium
733 (oxyhydr)oxides: Sorption-desorption of organic P on Al oxyhydroxides. *Eur J Soil Sci*
734 65, 308–317. <https://doi.org/10.1111/ejss.12119>
- 735